

---

## Mirror alignment and performance of the optical system of the H.E.S.S. imaging atmospheric Cherenkov telescopes

---

René Cornils,<sup>1</sup> Stefan Gillessen,<sup>2</sup> Ira Jung,<sup>2</sup> Werner Hofmann,<sup>2</sup> and Götz Heinzelmann,<sup>1</sup> for the H.E.S.S. collaboration

(1) Universität Hamburg, Institut für Experimentalphysik, Luruper Chaussee 149, D-22761 Hamburg, Germany

(2) Max-Planck-Institut für Kernphysik, P.O. Box 103980, D-69029 Heidelberg, Germany

---

### Abstract

The alignment of the mirror facets of the H.E.S.S. imaging atmospheric Cherenkov telescopes is performed by a fully automated alignment system using stars imaged onto the lid of the PMT camera. The mirror facets are mounted onto supports which are equipped with two motor-driven actuators while optical feedback is provided by a CCD camera viewing the lid. The alignment procedure, implying the automatic analysis of CCD images and control of the mirror alignment actuators, has been proven to work reliably. On-axis, 80% of the reflected light is contained in a circle of less than 1mrad diameter, well within specifications.

### 1. Introduction

H.E.S.S. is a stereoscopic system of large imaging atmospheric Cherenkov telescopes currently under construction in the Khomas Highland of Namibia [5]. The first two telescopes are already in operation while the complete phase 1 setup, consisting of four identical telescopes, is expected to start operation early 2004. The reflector of each telescope consists of 380 mirror facets with 60 cm diameter and a total area of 107 m<sup>2</sup>. For optimum imaging qualities, the alignment of the mirror facets is crucial. A fully automated alignment system has been developed, including motorized mirror supports, compact dedicated control electronics, various algorithms and software tools [1-3]. The specification for the performance of the complete reflector requires the resulting point spread function to be well below the size of a pixel of the Cherenkov camera.

### 2. Mirror alignment technique

The adjustable mirror unit consists of a support triangle carrying one fixed mirror support point and two motor-driven actuators. A motor unit includes the drive motor, two Hall sensors shifted by 90° sensing the motor revolutions and

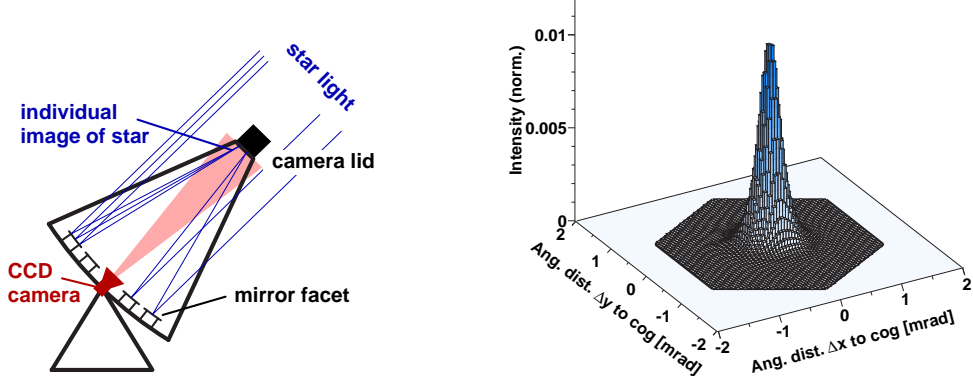


**Fig. 1.** *Left:* Mirror alignment technique. The telescope is pointed towards an appropriate star whereupon all mirror facets generate individual images of this star in the focal plane. Actuator movements change the location of the corresponding image which is observed by a CCD camera. *Right:* On-axis intensity distribution of a star on the camera lid after alignment. The hexagonal border indicates the size of a pixel of the PMT camera defined by the shape of the Winston cones.

providing four TTL signals per turn, and a 55:1 worm gear. The motor is directly coupled to a 12 mm threaded bolt, driving the actuator shaft by 0.75 mm per revolution. One count of the Hall sensor corresponds to a step size of  $3.4 \mu\text{m}$ , or 0.013 mrad tilt of the mirror. The total range of an actuator is about 28 mm which corresponds to  $6.15^\circ$  tilt of the mirror facet.

The alignment uses the image of an appropriate star on the closed lid of the PMT camera. The required optical feedback is provided by a CCD camera at the center of the dish, which is viewing the lid as illustrated in Fig. 1 (left). Individual mirror facets are adjusted such that all star images are combined into a single spot at the center of the PMT camera. The basic algorithm is as follows: a CCD image of the camera lid is taken. The two actuators of a mirror facet are then moved one by one, changing the location of the corresponding spot on the lid. These displacements are recorded by the CCD camera and provide all information required to subsequently position the spot at the center of the main focus. This procedure is repeated for all mirror facets in sequence.

It is – to our knowledge – the first time that such a technique is used to align the mirrors of Cherenkov telescopes. The major advantages of this approach are evident: a natural point-like source at infinite distance is directly imaged in the focal plane, and the alignment can be performed at the optimum elevation.

### 3. Point spread function

Fig. 1 (right) shows a CCD image of the image of a star on the camera lid after the alignment of all mirror facets in relation to the size of a PMT pixel ( $0.16^\circ$

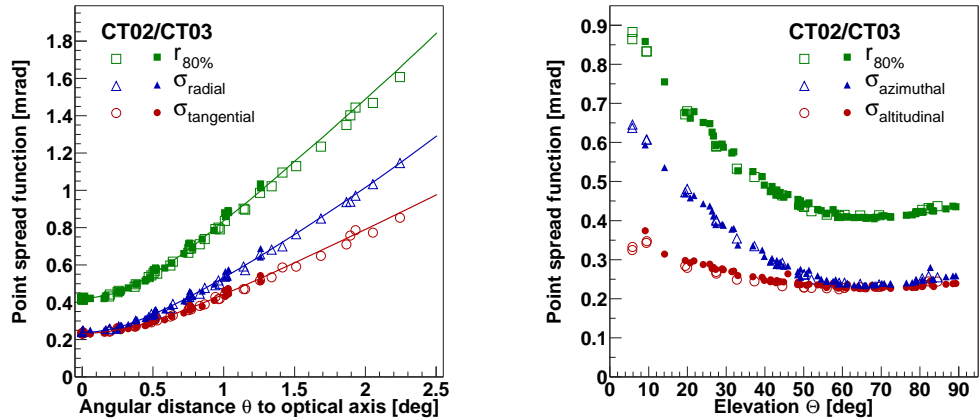


**Fig. 2.** Point spread function of the first two operational H.E.S.S. telescopes (CT03 and CT02). *Left:* Width of the point spread function as a function of the angular distance  $\theta$  to the optical axis at elevations around  $65^\circ$ . *Right:* Width of the point spread function as a function of telescope elevation  $\Theta$ .

diameter). The intensity distribution represents the on-axis point spread function for telescope elevations within the range used for the alignment ( $55^\circ$ – $75^\circ$ ). The distribution is symmetrical without pronounced substructure and the width of the spot is well below the PMT pixel size.

To parameterize the width of the intensity distributions, different quantities are used: the rms width  $\sigma_{proj}$  of the projected (1-dimensional) distributions and the radius  $r_{80\%}$  of a circle around the center of gravity of the image, containing 80% of the total intensity. On the optical axis, the point spread function is characterized by the values  $\sigma_{proj} = 0.23$  mrad and  $r_{80\%} = 0.41$  mrad (requirements:  $\leq 0.5$  and  $\leq 0.9$  mrad, respectively). This is an excellent result.

### 3.1. Variation of the point spread function across the field of view

Optical aberrations are significant in Cherenkov telescopes due to their single-mirror design without corrective elements and their modest  $f/d$  ratios. At some distance from the optical axis, the width of the point spread function is therefore expected to grow linearly with the angle  $\theta$  to the optical axis. For elevation angles around  $65^\circ$ , where the mirror facets were aligned, Fig. 2 (left) summarizes the spot parameters as a function of the angle  $\theta$ . Besides  $r_{80\%}$ , the rms widths of the distributions projected on the radial ( $\sigma_{\text{radial}}$ ) and tangential ( $\sigma_{\text{tangential}}$ ) directions are given. The measurements demonstrate that the spot width primarily depends on  $\theta$ ; no other systematic trend has been found and the width  $r_{80\%}$  is well described by

$$r_{80\%} = (0.42^2 + 0.71^2 \theta^2)^{1/2} \quad [\text{mrad}]. \quad (1)$$

To verify that the measured intensity distribution is quantitatively un-

derstood, Monte Carlo simulations of the actual optical system were performed, including the exact locations of all mirrors, shadowing by camera masts, the measured average spot size of the mirror facets, and the simulated precision of the alignment algorithm. The results are included in Fig. 2 (left) as solid lines, and are in good agreement with the measurements:

$$r_{80\%} = (0.42^2 + 0.72^2 \theta^2)^{1/2} \quad [\text{mrad}]. \quad (2)$$

### 3.2. Variation of the point spread function with telescope pointing

At fixed elevation, no significant dependence of the point spread function on telescope azimuth was observed. In contrast, a variation with elevation is expected due to gravity-induced deformations of the telescope structure. Fig. 2 (right) illustrates how the spot widths  $r_{80\%}$ ,  $\sigma_{\text{azimuthal}}$ , and  $\sigma_{\text{altitudinal}}$  change with elevation  $\Theta$ . The width  $r_{80\%}$  is to a good approximation described by

$$r_{80\%} = (0.41^2 + 0.96^2 (\sin \Theta - \sin 66^\circ)^2)^{1/2} \quad [\text{mrad}]. \quad (3)$$

For elevations most relevant for observations, i.e. above  $45^\circ$ , the spot size  $r_{80\%}$  varies by less than 10%. At  $30^\circ$  it is about 40% larger than the minimum size but still well below the size of the PMT pixels. A detailed analysis of the deformation of the support structure [2,4] revealed that the stiffness is slightly better than initially expected from finite element simulations.

## 4. Conclusion

The mirror alignment of the first two H.E.S.S. telescopes was a proof of concept and a test of all technologies involved: mechanics, electronics, software, algorithms, and the alignment technique itself. All components work as expected and the resulting point spread function significantly exceeds the specifications. Both reflectors behave almost identical which demonstrates the high accuracy of the support structure and the reproducibility of the alignment process.

## References

1. Bernlöhr K., Carrol O., Cornils R., Elfahem S. et al. 2003, The optical system of the H.E.S.S. imaging atmospheric Cherenkov telescopes, Part I, accepted
2. Cornils R., Gillessen S., Jung I., Hofmann W. et al. 2003, The optical system of the H.E.S.S. imaging atmospheric Cherenkov telescopes, Part II, accepted
3. Cornils R., Jung I. 2001, Proc. of the 27th Int. Cosmic Ray Conf., eds. Simon M., Lorenz E., and Pohl M. (Copernicus Gesellschaft), vol. 7, p2879
4. Cornils R., Gillessen S., Jung I., Hofmann W., Heinzelmann G. 2002, to appear in The Universe Viewed in Gamma-Rays, (Universal Academy Press)
5. Hofmann W. 2003, these proceedings